CHEMBIOCHEM

Enantiocomplementary Enzymatic Resolution of the Chiral Auxiliary: *cis,cis*-6-(2,2-Dimethylpropanamido)spiro[4.4]nonan-1-ol and the Molecular Basis for the High Enantioselectivity of Subtilisin Carlsberg

Paul F. Mugford,[a, c] Susan M. Lait,[b] Brian A. Keay,[b] and Romas J. Kazlauskas*[a, c]

*cis,cis-(±)-6-(2,2-Dimethylpropanamido)spiro[4.4]nonan-1-ol, **1**, a chiral auxiliary for Diels–Alder additions, was resolved by enzyme-catalyzed hydrolysis of the corresponding butyrate and acrylate esters. Subtilisin Carlsberg protease and bovine cholesterol esterase both showed high enantioselectivity in this process, but favored opposite enantiomers. Subtilisin Carlsberg favored esters of (1S,5S,6S)-**1**, while bovine cholesterol esterase favored esters of (1R,5R,6R)-**1**, consistent with the approximately mirror-image arrangement of the active sites of subtilisins and lipases/esterases. A gram-scale resolution of **1**-acrylate with subtilisin Carlsberg yielded (1S,5S,6S)-**1** (1.1 g, 46% yield, 99% ee) and (1R,5R,6R)-**1**-acrylate (1.3 g, 44% yield, 99% ee) although the reaction was slow. The high enantioselectivity combined with the conformational rigidity of the substrate made this an ideal example to identify the molecular basis of the enantioselectivity of subtilisin Carlsberg toward secondary alcohols. When modeled, the favored (1S,5S,6S) enantiomer adopted a catalytically productive conformation with two longer-than-expected hydrogen bonds, consistent with the slow reaction rate. The unfavored (1R,5R,6R) enantiomer encountered severe steric interactions with catalytically essential residues in the model. It either distorted the catalytic histidine position or encountered severe steric strain with Asn155, an oxyanion-stabilizing residue.*

Introduction

The enantiomer preference (which enantiomer is favored) is a key characteristic of enantioselective catalysts. For asymmetric syntheses, desymmetrizations, and dynamic kinetic resolutions, the enantiomer preference of the catalyst determines which enantiomer forms. Since most applications (for example, preparation of a pharmaceutical or pharmaceutical precursor) require only one enantiomer, it is important that the enantiomer formed is the desired one. Although kinetic resolutions yield both enantiomers, the enantiomer preference still determines which enantiomer will be the unreacted starting material and which will be the product of the reaction. This discrimination can simplify the next synthetic steps or, in a moderately enantioselective kinetic resolution, give higher enantiomer purity because the remaining starting material can be recovered in higher enantiomeric purity than the product.[1]

To reverse the enantiomer preference of a chemical catalyst, one uses the enantiomeric catalyst, for example, a D-tartrate-derived epoxidation catalyst in place of an L-tartrate-derived catalyst. For enzymes, the switch to an enantiomeric form is possible but not practical because it requires chemical synthesis of the enzyme from D-amino acids.[2] The practical solution for enzyme-catalyzed reactions is to use an enantiocomplementary enzyme, that is, one that favors the opposite enantiomer. Enantiocomplementary enzymes favor opposite enantiomers because either the substrate or the active-site machinery is oriented differently.

Researchers have discovered many examples of enantiocomplementary enzymes. For example, dehydrogenases as well as yeast reductases with opposite stereopreferences are common.[3,4] In *Escherichia coli*, separate enantiocomplementary enzymes reduce the enantiomeric sulfoxide configurations in methionine sulfoxide epimers.[5] In *Neisseria gonorrhoeae*, one protein, containing mirror-image active sites in separate domains, reduces these enantiomeric sulfoxide configurations.[6] In an oxidation example, the active site of D-amino acid oxidase is a mirror image of that in flavocytochrome-b_2. Both enzymes catalyze amino acid oxidation, but with opposite enantiomer preference.[7] Toluene dioxygenase and naphthalene dioxygenase are enantiocomplementary.[8] Researchers

[a] P. F. Mugford, Dr. R. J. Kazlauskas
McGill University, Department of Chemistry
801 Sherbrooke Street West, Montréal, Québec, H3A 2K6 (Canada)
[b] S. M. Lait, Dr. B. A. Keay
University of Calgary, Department of Chemistry
2500 University Drive, Calgary, Alberta, T4N 1N4 (Canada)
[c] P. F. Mugford, Dr. R. J. Kazlauskas
Current address:
Department of Biochemistry, Molecular Biology and Biophysics
University of Minnesota, and The Biotechnology Institute
1479 Gortner Avenue 174 Gortner Lab
St. Paul, MN 55108 (USA)
Fax: (+1) 612-625-5780
E-mail: rjk@umn.edu

  DOI: 10.1002/cbic.200300909 ChemBioChem 2004, 5, 980 – 987

reported diastereocomplementary aldolases[9] and enantiocomplementary aldolase catalytic antibodies.[10] Enantiocomplemtary pinene synthases cyclize geranyl diphosphate to give either (+)-(3*R*,5*R*)-α-pinene or (−)-(3*S*,5*S*)-α-pinene.[11] Researchers have also used protein engineering to reverse the enantioselectivity of enzymes.[12]

Enantiocomplementary hydrolases include esterases, lipases, and proteases,[13] epoxide hydrolases,[14] hydantoinases,[15] and lactamases.[16] Serine proteases and lipases have approximately mirror-image active sites and thus usually prefer opposite enantiomers of secondary alcohols and primary amines (Figure 1).[17] In this paper, we report the enantiocomplementary resolution of a secondary alcohol that is useful as a chiral auxiliary by using subtilisin Carlsberg or cholesterol esterase.

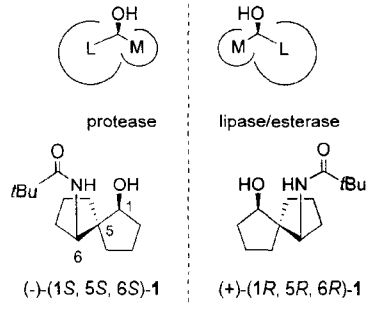

Figure 1. *Empirical rule to predict the fast-reacting enantiomer in hydrolysis reactions. M represents a medium-size substituent—in* ***1*** *this corresponds to the C2 methylene group. L represents a large substituent—in* ***1*** *this corresponds to the C5 spiro center.*

The *cis,cis*-1,3-amino alcohol **1** is an excellent chiral auxiliary for the Diels–Alder reaction because it shows excellent stereocontrol and high reactivity and it is easily removed. The acrylate of **1** forms a Diels–Alder adduct with cyclopentadiene in >98% *de* with an *endo*:*exo* ratio of >99:1 (Scheme 1).[18] In

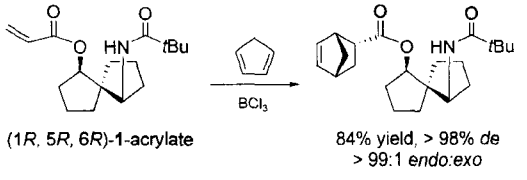

Scheme 1. *The highly diastereoselective Diels–Alder addition of cyclopentadiene to (1R,5R,6R)-1-acrylate.*

addition, it reacts with the less reactive dienes isoprene, furan, 1-vinylcyclopentene, and 1-vinylcyclohexane with good diastereoselectivities and yields. Removal of auxiliaries linked through an amide bond can be difficult, but the ester link of this auxiliary cleaves readily by saponification.

The synthesis of racemic **1** controls the relative configuration of the three stereocenters to give the *cis,cis* stereoisomer.[18] Fractional crystallization of the amine precursor of **1** (lacking the *N*-pivaloyl group) as the mandelate salt provided pure enantiomers with a yield of only 28% for each enantiomer, plus 28% recovered starting material. Here we report a kinetic resolution of (±)-**1** by two enantiocomplementary enzymes, both with an enantioselectivity greater than 200.

Results

We screened approximately 100 commercially available hydrolases for their ability to catalyze hydrolysis of racemic **1**-acetate. For the initial screen, we used *p*-nitrophenol as a pH indicator to detect proton release upon hydrolysis.[19] At the second stage, we monitored reactions on a scale of 1–5 mg by using gas chromatography. This screening identified only two hydrolases that catalyzed hydrolysis of **1**-acetate—subtilisin Carlsberg (or protease from *Bacillus licheniformis*) and proteinase N from *Bacillus subtilis* (Table 1). Even these two hydrolases were inefficient catalysts as the mass of enzyme required was 12–19 times higher than the mass of substrate. Subtilisin Carlsberg was approximately four times faster than proteinase N. The slow reaction with these two hydrolases and the inability of most hydrolases to catalyze hydrolysis of **1**-acetate is probably due to the rigid and hindered nature of this substrate.

Even though it showed no activity in the initial screen, we also checked the ability of bovine cholesterol esterase (CE) to catalyze hydrolysis of **1**-acetate because this esterase had previously resolved several spiro compounds.[20] We expected the reaction, if any, to be slow. Indeed, the reaction was very slow—with a 14-fold greater mass of esterase than of substrate, the reaction reached 36% conversion after 30 h. Even after 110 h it did not proceed beyond 38% conversion. It is possible that our screen missed other slow-reacting enzymes. However, we had identified three hydrolases that could catalyze hydrolysis of this unnatural substrate.

All three hydrolases showed an excellent enantiomeric ratio, *E* (Table 1). We calculated the enantioselectivity of the candidate enzymes from the enantiomeric purity measured by gas chromatography on a chiral stationary phase. For **1**-acetate, subtilisin Carlsberg gave an *E* value greater than 200 while proteinase N gave an *E* value of 100. CE was also highly enantioselective towards **1**-acetate with an *E* value greater than 200. The absolute configuration of the favored enantiomer was determined by comparison with a sample of **1** with known configuration.[18,21] The two proteases favored esters of (1*S*,5*S*,6*S*)-**1**, while CE favored esters of (1*R*,5*R*,6*R*)-**1**. This opposite enantiopreference is consistent with the secondary alcohol rules for proteases and lipases/esterases (see Figure 1 above). The two proteases and CE are enantiocomplementary enzymes and all show high enantioselectivity.

We tested the resolution of the **1**-butyrate ester, since separation of the starting material and the ester by column chromatography is easier with **1**-butyrate than with **1**-acetate, and also tested the resolution of **1**-acrylate since this yields the reactant for the Diels–Alder addition directly (Table 1). Upon changing the acetate to a butyrate or acrylate, the enantioselectivity remained unchanged. The rate for the acetate and

Table 1. Enzymatic resolution of esters of (±)-1.

Enzyme	Ester	t [h]	Enzyme/ester ratio[a]	ee_S[b,c] (yield)[d]	ee_P[b] (yield)[e]	Conv. [%][f]	E[g,h]
subtilisin Carlsberg	acetate[i]	48	12[j]	37	99	27	>200 (*S*)
from	butyrate[i]	24	1.7	89	99	47	>200 (*S*)
Bacillus licheniformis	acrylate	48	1.5	99 (44%)	99 (46%)	50	>200 (*S*)
proteinase N from	acetate	46	19[j]	20	98	17	100 (*S*)
Bacillus subtilis	butyrate	96	3.9	69	96	42	102 (*S*)
cholesterol esterase	acetate	30	14[j]	55	99	36	>200 (*R*)
	butyrate	24[k]	2.6	61	98	38	>200 (*R*)

[a] Ratio of mass of enzyme to mass of ester of (±)-**1**. [b] The measured *ee* values of the product and substrate, ee_P and ee_S,respectively, as determined by GC analysis. [c] The ee_S value for the butyrate was determined after column chromatography and hydrolysis to the alcohol **1**. [d] Yield of **1**-acrylate after isolation. [e] Yield of **1** after isolation. [f] The conversion [%] was determined from the ee_S and ee_P values by the formula $conv. = ee_S/(ee_S+ee_P)$. [g] The enantiomeric ratio, *E*, measures the relative rate of hydrolysis of the fast-reacting enantiomer as compared to the slow-reacting enantiomer, according to Equation (1). [h] The absolute configuration was determined by comparison to an authentic sample of (1*R*,5*R*,6*R*)-**1**.[18,21] [i] The rate of reaction for **1**-acetate should not be compared with the rates for **1**-butyrate/acrylate as the reactions were performed under different conditions. [j] When the amount of enzyme is more than twice the weight of substrate, Michaelis–Menten kinetics and the equations used to calculate enantioselectivity may not be valid because the molar amount of enzyme is no longer negligible compared to the amount of substrate. Nevertheless, the high enantiomeric purity of the product and experiments with smaller amounts of enzyme clearly indicate that the enantioselectivity is high. [k] This reaction was performed at 37 °C; the other butyrate reactions were performed at 25 °C.

butyrate/acrylate reactions in Table 1 should not be compared as these reactions were under different conditions. Butyrate reactions were carried out on a slightly larger scale (20 mg) and the relative amount of enzyme was reduced. Again we found that a high conversion could not be obtained with CE and the reaction temperature of 37 °C was crucial for any reaction with this enzyme. In contrast the subtilisin-catalyzed hydrolysis of **1**-butyrate proceeded to 47% conversion in 24 h at room temperature.

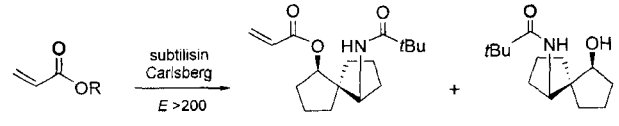

Scheme 2. Preparative-scale resolution of 1-acrylate with subtilisin Carlsberg.

For a practical resolution, we chose the subtilisin-catalyzed hydrolysis of **1**-acrylate (Scheme 2). Subtilisin Carlsberg is stable and inexpensive and this reaction directly yields the reactant needed for the subsequent Diels–Alder reaction. A 2.6-g resolution with subtilisin Carlsberg (4.3 g) in approximately 600 mL of buffer reached 50% conversion after 48 h at room temperature. Isolation and separation by column chromatography yielded unreacted (1*R*,5*R*,6*R*)-**1**-acrylate in 44% yield and 99% *ee* and product (1*S*,5*S*,6*S*)-**1** in 46% yield and 99% *ee*.

Molecular basis for the high enantioselectivity of subtilisin Carlsberg toward 1-butyrate

Starting with the X-ray crystal structure of subtilisin Carlsberg, we added **1**-butyrate to the active site by using computer modeling.[22] We further replaced the reacting ester carbonyl moiety of **1**-butyrate with a phosphonate group to mimic the transition state (Scheme 3a) and linked this phosphonate group to the catalytic serine residue. The chiral alcohol moiety has only a few accessible conformations because it has only three rotatable bonds and its large size excludes many conformations within the active-site pocket. We manually searched conformations by rotating the P–O bond, the O–C1 bond, and the C6–N bond. Catalytically productive structures were those that contained all five catalytically essential hydrogen bonds (Scheme 3b) and avoided steric clashes with the protein.

The phosphonate structure mimicking hydrolysis of the fast-reacting (1*S*,5*S*,6*S*) enantiomer adopted a catalytically productive orientation (Scheme 3b) but the alcohol substituents made little contact with the substrate-binding site. The alcohol moiety rested above the active site with the medium substituent (the C2 methylene,see Figure 1) slightly above the right side of the shallow S_1' binding site (defined by Met222, yellow, at the bottom, Leu217, red, on the left, and the backbone of Asn218, green, on the right in Figure 2 l). The large substituent (the C5 spiro center and ring, see Figure 1) was unbound and pointed toward the solvent (to the left in Figure 2 l). The closest contact between the medium substituent and the S_1' binding site was longer than the van der Waals contact distance (4.52 Å between the C3 atom of the **1** moiety and the sulfur atom of Met222 versus 4.09 Å[23] for a van der Waals contact). But this distance is close enough to exclude water and create a favorable hydrophobic interaction. Thus, the substituents in the alcohol moiety were only partly in the substrate-binding site.

Two of the catalytically essential hydrogen bonds were longer than expected. The alcohol orientation pointed the alcohol oxygen atom toward the catalytic histidine residue to form a hydrogen bond. This bond was longer than expected: the Nε2–O distance was 3.33 Å and the N–H–O angle was 135°, while the normal limits for a hydrogen bond are ≈3.1 Å length and an angle greater than 120°. The hydrogen bond from the His64 Nε2 atom to the Ser221 Oγ atom was also longer than expected at 3.42 Å (N–H–O angle of 133°). These two long hydrogen bonds may explain the very slow reaction for this substrate.[24]

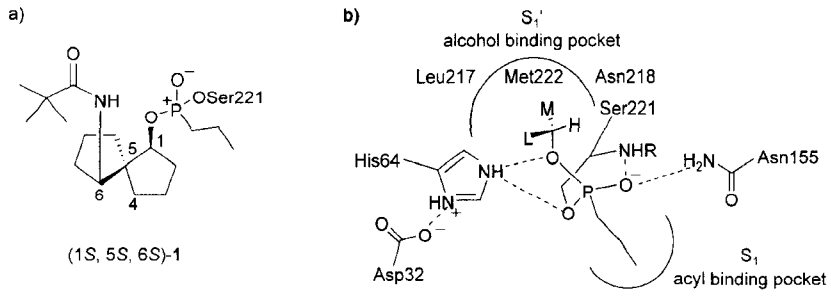

Scheme 3. a) Phosphonate transition-state analogue derived from the fast-reacting (1S,5S,6S)-1-butyrate. b) Key hydrogen bonds between the phosphonate group and the catalytic residues of subtilisin Carlsberg.

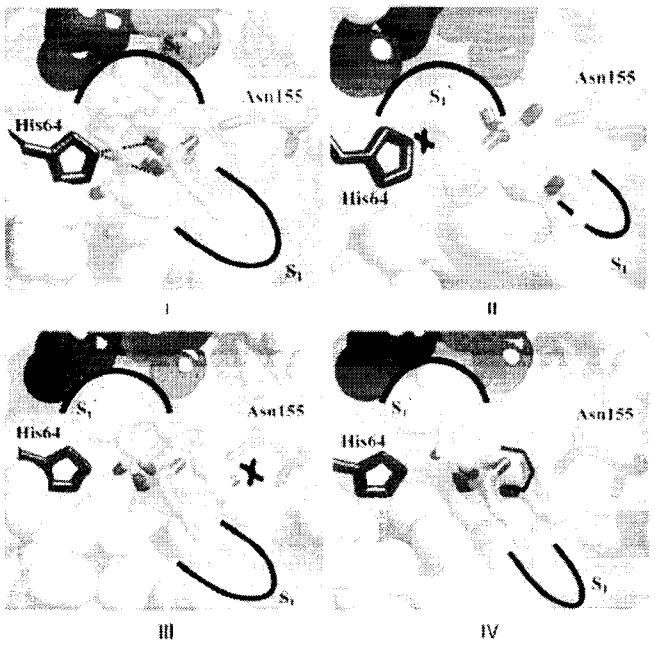

Figure 2. *Geometry-optimized conformations of the tetrahedral intermediates for hydrolysis of 1-butyrate in the active site of subtilisin Carlsberg. The residues defining the S_1' site are Met222 (yellow), Leu217 (dark red), and Asn218 (green). I) The catalytically productive conformation of the fast-reacting enantiomer (1S,5S,6S)-1-butyrate. Three nonproductive conformations of the slow-reacting enantiomer (1R,5R,6R)-1-butyrate: II) Conformation A is missing key hydrogen bonds because of the distorted histidine orientation, III) conformation B has several distorted bond angles as a result of steric interactions with Asn155, and IV) conformation C has a syn-pentane-like interaction and several other distorted bond angles.*

We examined three different conformations for the slow-reacting (1*R*,5*R*,6*R*) enantiomer, but they either lacked key hydrogen bonds or encountered severe steric clash with the protein. The first conformation for the (1*R*,5*R*,6*R*) enantiomer (Figure 2 II, conformation A) had a severely distorted histidine orientation. It placed the medium substituent of **1** into the left side of the shallow S_1' pocket (deeper than the fast-reacting enantiomer); the distance from the C3 atom to the sulfur atom of Met222 was 4.20 Å. The large substituent pointed directly out of the active site and toward the solvent. The different absolute configuration of the alcohol stereocenter pointed the alcohol oxygen atom away from the catalytic histidine residue. In addition, the medium substituent hit the catalytic histidine, thereby causing the plane of the imidazole ring to rotate down into the active site by 60° (as compared with the fast-reacting enantiomer). The resulting distance between the C2 atom of the substrate and the Nε2 atom of His64 was 3.44 Å. This shift severely disrupted all three of the catalytically essential hydrogen bonds involving the catalytic histidine residue (Table 2). The distance from the His64 Nε2 atom to the Ser221 Oγ atom was too long form a hydrogen bond (4.04 Å, N–H–O angle of 124°), as was the distance to the alcohol oxygen atom (5.17 Å, N–H–O angle of 96°). Although the distance between the Asp32 Oδ atom and the His64 Nδ1 atom remained small (2.95 Å), the O–H–N angle decreased to 66°, which is too acute to form a hydrogen bond. These disruptions of the catalytic-hydrogen-bond network make it extremely unlikely that the slow-reacting enantiomer could react through conformation A.

In the second slow-reacting (1*R*,5*R*,6*R*) conformation (conformation B), the alcohol moiety rotated clockwise along the P–O bond to relieve the histidine distortion and restore the catalytically essential hydrogen bonds (Table 2). This rotation placed the medium substituent above the left side of the S_1' pocket and the closest distance was significantly longer than the van der Waals contact distance (5.06 Å between the C3 atom and the sulfur atom of Met222). This rotation also pointed the large group to the right (from the perspective of Figure 2 III) where its bulky pivalamide group hit the side of the active site at Asn155. Asn155 also has a catalytic role—the $N_\alpha H$ group stabilizes the oxyanion of the transition state by forming a hydrogen bond. The pivalamide carbonyl group made hydrogen bonds to the NH_2 ($N_{\delta 2}$) group of Asn155 (N–O distance of 2.92 Å, O–H–N angle of 163°) and to the backbone NH (N_α) group (3.07 Å, N–H–O angle of 125°), as well as a close steric contact with the β-carbon atom (3.27 Å). This pivalamide–Asn155 contact also distorted bond angles in the alcohol moiety: the P–O–C1 angle was 128°, rather than 120° as in the ideal case, and the O–C1–C5 angle was 116° instead of 109° (Table 3). Restoring these two angles to their ideal values dramatically increased the steric interactions between the pivalamide carbonyl group and Asn155 (distances: $N_{\delta 2}$–O = 2.29 Å, N_α–O = 3.04 Å, and C_β–O = 2.54 Å). To confirm that conformation B is a strained conformation, we calculated its energy (AM1, heat of formation) after removal from subtilisin

Table 2. *Lengths and angles of catalytically essential hydrogen bonds as determined by molecular modeling.*[a]

	Hydrogen-bond length [Å] (angle)			
	(1*S*,5*S*,6*S*)	(1*R*,5*R*,6*R*)		
		conformation A	conformation B	conformation C
His64–$O_{alcohol}$	3.33 (135°)	**5.17 (96°)**	3.30 (146°)	3.30 (147°)
His64–O_{Ser221}	3.42 (133°)	**4.04 (124°)**	3.36 (137°)	3.39 (138°)
oxyanion–NH_{Ser221}	2.80 (154°)	2.72 (159°)	2.86 (149°)	2.85 (151°)
oxyanion–$NH_{2\,Asn155}$	2.79 (164°)	2.78 (129°)	2.76 (128°)	2.75 (140°)
Asp32–His64	2.76 (162°)	2.95 (66°)	2.78 (173°)	2.78 (174°)
conclusions	productive conformation	key hydrogen bonds missing	high-energy structure	*syn*-pentane-like interaction

[a] Bold font indicates distances that are too long to form a hydrogen bond.

Table 3. *Energy of substrate and substrate angles for tetrahedral intermediates.*

	(1*S*, 5*S*, 6*S*)	(1*R*, 5*R*, 6*R*) conformation		
		A	B	C
heat of formation[a] [kcal mol^{-1}]	0	+2	+16	+17
C1–C5–C4	102°	103°	100°	99°
C1–C5–C6	116°	116°	117°	119°
C1–C5–C9	113°	113°	116°	117°
N–C6–C5[b]	112°	110°	110°	**117°**
O–C1–C5[b]	109°	109°	**116°**	**116°**
P–O–C1[b]	122°	123°	**127°**	**128°**

[a] AM1 heat of formation of the substrate removed from subtilisin. [b] Bold font indicates bond angles distorted from their ideal values. Restoring the angles in bold font to their ideal values in conformations B and C gave severe steric clashes with the Asn155 residue.

Carlsberg and found this to be 16 kcal mol^{-1} higher than the energy of the conformation for the fast-reacting enantiomer. In summary, although conformation B contains the catalytically essential hydrogen bonds, steric clash between the pivalamide carbonyl group and Asn155 make this a highly strained conformation.

Rotation of the pivalamide group along the C6–N bond to avoid the steric clashes with Asn155 yields conformation C. Unfortunately, this rotation creates a new steric strain—a *syn*-pentane-like interaction between the oxygen atom of the pivalamide moiety and the spiro stereocenter (O–C5 distance of 3.00 Å, Figure 2 IV). Typically a *syn*-pentane interaction increases the energy by ≈3.6 kcal mol^{-1}.[25] The main close contact with the enzyme was between the pivalamide NH group and the NH_2 group of Asn155 (3.16 Å). The significantly distorted angles in this structure were the N–C6–C5 angle (117°), the P–O–C1 angle (128°), and the O–C1–C5 angle (116°, Table 3). Restoring these angles to their ideal values dramatically shortened the distance from the NH group of the pivalamide to the NH_2 group of Asn155 (2.51 Å). The calculated energy of the transition-state analogue removed from the protein was 17 kcal mol^{-1} higher than the fast-reacting enantiomer, a result indicating that this conformation is highly strained.

Discussion

Two enantiocomplementary enzymes—subtilisin and cholesterol esterase—show high enantioselectivity toward esters of (±)-**1**. The favored enantiomer for both follows the secondary alcohol rules developed to predict the enantioselectivity of serine hydrolases.[17] Kim and co-workers also recently used subtilisin and lipases as enantiocomplementary enzymes in the dynamic kinetic resolution of secondary alcohols.[26]

The gram-scale resolution of **1**-acrylate with subtilisin gave high yield and enantiomeric purity but was very slow. We used a mass of subtilisin 1.7 times higher than the mass of substrate. Nevertheless, this resolution is a practical procedure because subtilisin Carlsberg is an inexpensive enzyme (US $12 per gram from Sigma). In addition, subtilisin Carlsberg is stable and could be reused. Given the bulky nature of this substrate, it is not surprising that it might react slowly. Other bulky substrates such as esters of α-branched amino acids also reacted slowly with subtilisin Carlsberg.[27] The advantage of this procedure over resolution by crystallization of the amine precursor as the mandelate salt is that this kinetic resolution yields the desired acrylate ester directly.

Subtilisin Carlsberg usually shows only low to moderate enantioselectivity toward secondary alcohols, but in this case the enantioselctivity is very high. Molecular modeling revealed the molecular basis for this high enantioselectivity. The fast-reacting (1*S*,5*S*,6*S*) enantiomer fits in the active site and makes all five catalytically essential hydrogen bonds, although two of these are longer than normal, which probably explains the low reactivity for the substrate. On the other hand, the slow-reacting (1*R*,5*R*,6*R*) enantiomer encounters severe steric interactions with catalytically essential residues. These interactions either distort the catalytic histidine position or cause severe steric strain with Asn155, an oxyanion-stabilizing residue.

Ema and co-workers proposed an alternative explanation for the enantioselectivity of lipases[28] and subtilisin[29] toward secondary alcohols. They suggest that the fast-reacting enantiomer adopts a conformation where stereoelectronic effects favor reaction, while the slow-reacting enantiomers cannot adopt this conformation. Thus, the fast-reacting enantiomer should adopt a *gauche* (*g*− for proteases) conformation along the $C_{alcohol}$–$O_{alcohol}$–$C_{C=O}$–Oγ dihedral, thereby allowing overlap of the antiperiplanar lone-pair orbital of the $O_{alcohol}$ atom with the σ* orbital of the breaking C–Oγ bond. They propose that the slow-reacting enantiomer cannot adopt this favorable orientation because the large substituent would hit the catalytic histidine residue.

Our modeling does not support this proposal because the fast-reacting enantiomer cannot adopt a *gauche* orientation along the $C_{alcohol}$–$O_{alcohol}$–$C_{C=O}$–Oγ dihedral. The fast-reacting enantiomer adopted an *anti* conformation along this bond

(−172°) in order to make the catalytically essential hydrogen bonds. Imposing a *gauche* conformation (−60°) along this dihedral caused a severe steric clash between the medium substituent (C2) and His64 (1.78 Å, with the C1 hydrogen atom *syn* to the oxyanion). The slow-reacting enantiomer, predicted to adopt an *anti* conformation by the stereoelectronic effects model, indeed adopted the *anti* conformation in conformations B (151°) and C (159°); however, because the orientation is also *anti* for the fast-reacting enantiomer, it cannot contribute to enantioselectivity. Conformation A of the slow-reacting enantiomer adopted a *gauche* conformation, (63°, g+ rather than *g*−) but still hit the catalytic residue His64. Thus, we find no evidence to support the notion that stereoelectronic effects along the $C_{alcohol}$–$O_{alcohol}$–$C_{C=O}$–Oγ dihedral contribute to the enantioselectivity of subtilisin Carlsberg toward alcohol **1**.

Previous X-ray crystal structures of phosphonate transition-state analogues containing secondary alcohols also do not support the notion that stereoelectronic effects along the $C_{alcohol}$–$O_{alcohol}$–$C_{C=O}$–Oγ dihedral contribute to enantioselectivity. The fast-reacting enantiomer of menthol bound to a lipase from *Candida rugosa* did not adopt the predicted *gauche* conformation (130°).[30] On the other hand, the slow-reacting enantiomer did adopt a *gauche* conformation (71°), again contrary to predictions.

The X-ray crystal structures of bovine cholesterol esterase are only of inactive forms,[31] so we did not model their interactions with alcohol **1**.

Experimental Section

General: Chemicals were purchased from Sigma–Aldrich (Oakville, ON) and were used without further purification. Subtilisin from *Bacillus licheniformis* (EC 3.4.21.62) was obtained from Sigma (Oakville, ON; catalogue no. P5459) and proteinase N from *Bacillus subtilis* was obtained from Fluka (Oakville, ON; catalogue no. 82458). Cholesterol esterase from beef pancreas (EC 3.1.1.13) was obtained from Genzyme (Cambridge, MA; catalogue no. 1081).

Synthesis: The alcohol **1** and the acrylate ester were synthesized according to a previous method.[18] The **1**-acetate and **1**-butyrate were made by a similar method.

(±)-1-Acetate: (±)-**1** (62.0 mg, 0.259 mmol) and lithium hexamethyldisilanazide (LHMDS; 100 mg, 0.598 mmol) were dissolved in tetrahydrofuran (THF; 6 mL) and stirred for 1 h to give a gold-colored suspension. Acetic anhydride (60 μL, 0.64 mmol) was added and the solution was stirred for 16 h. The resulting gold solution was quenched with water (10 mL) then aqueous HCl (4 M, 10 mL) and extracted with CH_2Cl_2 (3×20 mL). The combined organic layers were washed with saturated aqueous Na_2CO_3 (20 mL) and dried over $MgSO_4$. Concentration in vacuo followed by flash column chromatography (silica, hexanes/EtOAc 4:1) gave (±)-**1**-acetate (47.6 mg, 0.169 mmol, 65.3%) as a white solid: M.p. 122–123 °C; $[\alpha]_D^{22}$ −47.2 (c = 1.08 in $CHCl_3$); IR (film): λ_{max} = 3328 (N–H), 2956 (C–H), 2873 (C–H), 1727 (ester C=O), 1625 (amide C=O), 1538 (C=C), 1373, 1245, 1100, 1016 cm^{-1}; ^{1}H NMR (400 MHz, $CDCl_3$): δ = 6.00 (br d, 1H, HN), 5.02–4.96 (m, 1H, H1), 4.28–4.20 (m, 1H, H6), 2.03 (s, 3H, H14), 2.05–1.45 (m, 12H, H2–H4, H7–H9), 1.16 (s, 9H, H12) ppm; ^{13}C NMR (100 MHz, $CDCl_3$): δ = 177.4 (C, C10), 170.4 (C, C13), 81.2 (CH, C1), 56.2 (CH, C6), 56.1 (C, C5), 38.7 (C, C11), 34.8 (CH_2), 34.7 (CH_2), 32.2 (CH_2), 31.8 (CH_2), 27.5 (CH_3, C12), 21.5 (CH_3, C14), 21.1 (CH_2), 20.2 (CH_2) ppm; MS: *m/z* (%): 281 (6) $[M]^+$, 238 (12) $[M-CH_3CO]^+$, 196 (30) $[M-(CH_3)_3CCO]^+$, 121 (64) $[M-\{(CH_3)_3CCONH_2+CH_3CO_2\}]^+$, 120 (100) $[M-\{(CH_3)_3CCONH_2+CH_3CO_2H\}]^+$, 102 (75) $[(CH_3)_3CCONH_3]^+$, 57 (86); HRMS: calcd for $C_{16}H_{27}NO_3$: 281.19909; found: 281.20062.

(±)-1-Butyrate: (±)-**1** (810 mg, 3.38 mmol) and LHMDS·OEt_2 (1.72 g, 7.12 mmol) were dissolved in THF (40 mL) and stirred for 1 h to give a gold-colored suspension. Butyryl chloride (750 μL, 7.22 mmol) was added and the solution was stirred for 1 h. The resulting clear yellow solution was quenched with water (20 mL) then aqueous HCl (4 M, 50 mL) and extracted with CH_2Cl_2 (3× 50 mL). The combined organic layers were washed with saturated aqueous Na_2CO_3 (50 mL) and dried over $MgSO_4$. Concentration in vacuo followed by flash column chromatography (silica, hexanes/EtOAc 4:1) gave (±)-**1**-butyrate (901 mg, 2.91 mmol, 86.1%) as a white solid: M.p. 107–108 °C; $[\alpha]_D^{22}$ −44.6 (c = 1.01 in $CHCl_3$); IR (film): λ_{max} = 3339 (N–H), 2962 (C–H), 2872 (C–H), 1730 (ester C=O), 1632 (amide C=O), 1537 (C=C), 1453, 1435, 1416, 1394, 1367, 1305, 1203, 1186, 1100, 994, 945 cm^{-1}; ^{1}H NMR (400 MHz, $CDCl_3$): δ = 6.04 (br d, 1H, HN), 5.01 (dd, J = 5.5, 2.5 Hz, 1H, H1), 4.26–4.18 (m, 1H, H6), 2.26 (t, J = 7.5 Hz, 2H, H14), 2.08–1.45 (m, 14H, H2–H4, H7–H9, H15), 1.16 (s, 9H, H12), 0.94 (t, J = 7.4 Hz, 3H, H16) ppm; ^{13}C NMR (100 MHz, $CDCl_3$): δ = 177.5 (C, C10), 172.9 (C, C13), 81.0 (CH, C1), 56.4 (CH, C6), 55.8 (C, C5), 38.7 (C, C11), 36.6 (CH_2), 35.0 (CH_2), 34.9 (CH_2), 32.4 (CH_2), 31.7 (CH_2), 27.6 (CH_3, C12), 21.1 (CH_2), 20.2 (CH_2), 18.4 (CH_2), 13.7 (CH_3, C16); MS: *m/z* (%): 309 (4) $[M]^+$, 238 (15) $[M-C_3H_7CO]^+$, 224 (35) $[M-(CH_3)_3CCO]^+$, 121 (64) $[M-\{(CH_3)_3CCONH_2+C_3H_7CO_2\}]^+$, 120 (100) $[M-\{(CH_3)_3CCONH_2+C_3H_7CO_2H\}]^+$, 102 (82) $[(CH_3)_3CCONH_3]^+$, 57 (78); HRMS: calcd for $C_{18}H_{31}NO_3$: 309.23039; found: 309.23114.

Identifying the active hydrolases: An enzyme library of commercial hydrolases was prepared as previously described.[19] Hydrolase solutions (20 μL per well) were placed in a 96-well microplate and assay solution (80 μL per well) was added. The final concentrations were 5.1 mM **1**-acetate, 3.6 mM *N,N*-bis(2-hydroxyethyl)-2-aminoethanesulfonic acid (BES), 0.36 mM 4-nitrophenol, and 8% acetonitrile. The plate was placed in the microplate reader and shaken for 10 s to ensure complete mixing, and the decrease in absorbance at 404 nm was then monitored at 25 °C every 11 s for 30 min. Each hydrolysis was carried out in triplicate and averaged. The normalized initial decrease in absorbance for the interval 20–300 s after initiation was −13 s^{-1} for subtilisin from *Bacillus licheniformis* (initial hydrolase solution of 22 mg mL^{-1}) and −6 s^{-1} for proteinase N (initial hydrolase solution of 60 mg mL^{-1}). These enzymes were then tested for enantioselectivity in small-scale reactions.

Measuring hydrolase enantioselectivity: BES buffer (450 μL, 50 mM, pH 7.2) and **1**-acetate (50 μL, 76 mM in MeCN) were placed in a 1.5-mL centrifuge tube along with enzyme (12–19 mg). Reactions were shaken at 600 rpm and 37 °C for 12 h in an Eppendorf Thermomixer R and then extracted with EtOAc (0.5 mL). The organic extract was dried with $MgSO_4$ and analyzed by gas chromatography on a Chrompack Chirasil-DEX CB column (25 m×0.25 mm) with He as the carrier gas (120 °C for 5 min then 2.5 °C min^{-1} increase up to 195 °C, 10 psi): **1**-acetate: k'_1 = 15.94 (*S*), α = 1.01; **1**: k'_1 = 17.10 (*R*), α = 1.02 (where k'_1 is the capacity factor given by $k'_1 = (t_{RT}-t_M)/t_M$ such that t_{RT} is the retention time of the sample and t_M is the dead time. α is the selectiveity factor given tby the ratio of the R and S capacity factors. For **1**-acetate, the (*S,S,S*) enantiomer elutes first while for the alcohol **1**, the (*R,R,R*) enantiomer elutes first. Both **1**-acetate and **1** showed similar retention during TLC (silica gel): R_f = 0.65 and 0.57, respectively, in hexanes/ethyl acetate (1:1). To measure the enantioselectivity of reactions involv-

ing **1**-butyrate, the remaining **1**-butyrate and product **1** were separated by TLC ($R_f = 0.81$ and 0.57, respectively, in hexanes/ethyl acetate (1:1)). The product **1** was analyzed by GC as above, but the enantiomers of **1**-butyrate did not separate under these conditions, so the **1**-butyrate was hydrolyzed to **1** with NaOH (1 mL, 6 M) in MeOH (4 mL) and extracted with EtOAc (2 mL). The organic extract was dried and the hydrolyzed product was then analyzed by GC as above. To measure the enantioselectivity of reactions involving **1**-acrylate, the remaining **1**-acrylate and product **1** were separated by chromatography (**1**-acrylate: $R_f = 0.77$ in hexanes/ethyl acetate (1:1)) and analyzed by GC (130 °C then 0.5 °C min^{-1} increase up to 185 °C, 10 psi): **1**-acrylate: $k'_1 = 34.71$ (*S*), $\alpha = 1.01$; **1**: $k'_1 = 34.62$ (*R*), $\alpha = 1.04$. Separation of **1**-acrylate and **1** was required because they overlap in the GC trace. The enantiomeric ratio, *E*, was calculated from the measured *ee* values of the product and substrate, ee_P and ee_S, respectively, according to:

$$E = \frac{\ln[ee_P(1-ee_S)/(ee_P+ee_S)]}{\ln[ee_P(1+ee_S)/(ee_P+ee_S)]} \quad (1)$$

as defined by Sih and co-workers.[32]

Resolution of 1-acrylate: Protease from *Bacillus licheniformis* (60 mL aqueous propylene glycol solution, 73 mg mL^{-1}, 9.1 U mg^{-1}) was placed in BES buffer (2 mM, 560 mL) and MeCN (25 mL), and the pH value was adjusted to 7.2 by using a pH stat. **1**-Acrylate (2.88 g, 98.2 mmol) in MeCN (25 mL) was then added and the pH value was maintained at 7.2 by the addition of NaOH (0.1 M). At 50% conversion, the reaction was extracted with EtOAc (3× 200 mL). The combined organic layers washed with water (200 mL) and brine (200 mL), then dried over $MgSO_4$. The solvent removed under reduced pressure. Separation by chromatography (hexanes/EtOAc (5:1)) yielded (1*S*,5*S*,6*S*)-**1** (1.07 g, 44.7 mmol, 46%, 99% *ee*) as a white solid (m.p. 102–104 °C) and (1*R*,5*R*,6*R*)-**1**-acrylate (1.27 g, 43.3 mmol, 44%, 99% *ee*) as a white solid (m.p. 126–127 °C).

Computer modeling: Molecular modeling was performed by using the Biosym/MSI InsightII 97.0/Discover software (San Diego, CA) with the Amber 95.0[33] force field. A distance-dependent dielectric constant of 4.0 was used and 1–4 van der Waals interactions were scaled by 50%. The starting subtilisin Carlsberg structure was obtained from the Brookhaven protein data bank[34] (file: 1cse).[22] The elgin c inhibitor was removed, hydrogens were added to correspond to a pH value of 7.0, and the catalytic histidine (His64) was protonated. Initial relaxation of the enzyme was performed with a simple phosphonate transition-state analogue. With the backbone constrained, 200 iterations of the steepest descent algorithm were performed, followed by 200 iterations of the conjugant gradients algorithm with the backbone tethered by a 10 kcal mol^{-1} Å^{-1} force constant, and finally by 200 iterations without any constraints. The substrate was then added and minimizations were performed in an analogous manner. Crystallographic water molecules were included in all minimizations. Final minimization was continued until the root mean square value was less than 0.0001 kcal mol^{-1}.

Acknowledgements

We thank the Natural Sciences and Engineering Research Council of Canada for financial support.

Keywords: chiral auxiliaries · enantioselectivity · hydrolases · kinetic resolution · molecular modeling

[1] K. Faber, *Biotransformations in Organic Chemsitry*, Springer, Berlin, **2000**, pp. 29–176.
[2] R. C. L. Milton, S. C. F. Milton, S. B. H. Kent, *Science* **1992**, *256*, 1445–1448; L. E. Zawadzke, J. M. Berg, *J. Am. Chem. Soc.* **1992**, *114*, 4002–4003; M. C. Fitzgerald, I. Chernushevich, K. G. Standing, S. B. H. Kent, C. P. Whitman, *J. Am. Chem. Soc.* **1995**, *117*, 11075–11080.
[3] M. Nakazaki, H. Chikamatsu, K. Naemura, T. Suzuki, M. Iwasaki, Y. Sasaki, T. Fujii, *J. Org. Chem.* **1981**, *46*, 2726–2730.
[4] G. Fantin, M. Fogagnolo, P. P. Giovannini, A. Medici, P. Pedrini, F. Gardini, R. Lanciotti, *Tetrahedron* **1996**, *52*, 3547–3552.
[5] F. Etienne, D. Spector, N. Brot, H. Weissbach, *Biochem. Biophys. Res. Commun.* **2003**, *300*, 378–382.
[6] W. T. Lowther, H. Weissbach, F. Etienne, N. Brot, B. W. Matthews, *Nat. Struct. Biol.* **2002**, *9*, 348–352.
[7] A. Matievi, M. A. Vanoni, F. Todone, M. Rizzi, A. Teplyakov, A. Coda, M. Bolognesi, B. Curti, *Proc. Natl. Acad. Sci. USA* **1996**, *93*, 7496–7501.
[8] N. I. Bowers, D. R. Boyd, N. D. Sharma, P. A. Goodrich, M. R. Groocock, A. J. Blacker, P. Goode, H. Dalton, *J. Chem. Soc. Perkin Trans. 1* **1999**, 1453–1461.
[9] D. P. Henderson, I. C. Cotterill, M. C. Shelton, E. J. Toone, *J. Org. Chem.* **1998**, *63*, 906–907.
[10] J. M. Turner, T. Bui, R. A. Lerner, C. Barbas, B. List, *Chem. Eur. J.* **2000**, *6*, 2772–2774.
[11] M. A. Phillips, M. R. Wildung, D. C. Williams, D. C. Hyatt, R. Croteau, *Arch. Biochem. Biophys.* **2003**, *411*, 267–276.
[12] a) O. May, P. T. Nguyen, F. H. Arnold, *Nat. Biotechnol.* **2000**, *18*, 317–320; b) E. Henke, U. T. Bornscheuer, R. D. Schmid, J. Pleiss, *ChemBioChem*, **2003**, *4*, 485–493; c) D. Zha, S. Wilensek, M. Hermes, K. E. Jaeger, M. T. Reetz, *Chem. Commum.* **2001**, 2664–2665; d)Y. Koga1, K. Kato, H. Nakano, T. Yam, *J. Mol. Biol.* **2003**, *331*, 585–592.
[13] a) G. de Gonzalo, R. Brieva, V. Sánchez, M. Bayod, V. Gotor, *J. Org. Chem.* **2003**, *68*, 3333–3336; b) H.-J. Gais, I. von der Weiden, J. Fleischhauer, J. Esser, G. Raabe, *Tetrahedron: Asymmetry* **1997**, *8*, 3111–3123; c) J. V. Allen, J. M. J. Williams, *Tetrahedron Lett.* **1996**, *37*, 1859–1862; d) A. Gentile, C. Giordano, *J. Org. Chem.* **1992**, *57*, 6635–6637; e) J. Z. Crich, R. Brevia, P. Marquart, R.-L. Gu, S. Flemming, C. J. Sih, *J. Org. Chem.* **1993**, *58*, 3252–3258.
[14] S. Mayer, A. Steinreiber, M. Goriup, R. Saf, K. Faber, *Tetrahedron: Asymmetry* **2002**, *13*, 523–528; b) K. C. Williamson, C. Morisseau, J. E. Maxwell, B. D. Hammock, *Tetrahedron: Asymmetry* **2000**, *11*, 4451–5562.
[15] J. Altenbuchner, M. Siemann-Herzberg, C. Syldatk, *Curr. Opin. Biotechnol.* **2001**, *12*, 559–563.
[16] C. Evans, R. McCague, S. M. Roberts, A. G. Sutherland, *J. Chem. Soc. Perkin Trans. 1* **1991**, 656–657.
[17] R. J. Kazlauskas, A. N. E. Weissfloch, A. T. Rappaport, L. A. Cuccia, *J. Org. Chem.* **1991**, *56*, 2656–2665; b) P. A. Fitzpatrick, A. M. Klibanov, *J. Am. Chem. Soc.* **1991**, *113*, 3166–3171; c) R. J. Kazlauskas, A. N. E. Weissfloch, *J. Mol. Catal. B* **1997**, 65–73.
[18] S. M. Lait, M. Parvez, B. A. Keay, *Tetrahedron: Asymmetry* **2003**, *14*, 749–756.
[19] L. E. Janes, A. C. Löwendahl, R. J. Kazlauskas, *Chem. Eur. J.* **1998**, *4*, 2324–2330.
[20] R. J. Kazlauskas, *J. Am. Chem. Soc.* **1989**, *111*, 4953–4959.
[21] M. J. Burke, M. M. Allan, M. Parvez, B. A. Keay, *Tetrahedron: Asymmetry*, **2000**, *11*, 2733–2739.
[22] W. Bode, E. Papamokos, D. Musil, *Eur. J. Biochem.* **1987**, *166*, 673–692.
[23] Estimated from the C–H bond length (1.09 Å) and van der Waals radii for sulfur (1.80 Å) and hydrogen (1.20 Å) from A. Bondi, *J. Phys. Chem.* **1964**, *68*, 441–451.
[24] Although nonproductive orientations may also exist for the fast-reacting enantiomer we did not consider them because only productive orientations lead to product. Nonproductive orientations only slow the rate of reaction. Nonproductive orientations alter the rate of reaction, k_{cat}, and the Michaelis constant, K_M, in a compensating manner, so that k_{cat}/K_M and the enantioselectivity are unaffected (A. Fersht, *Structure and Mechanism in Protein Science*, Freeman Freeman, New York, **1999**, pp. 114–117).
[25] E. L. Eliel, S. H. Wilen, *Stereochemistry of Organic Compounds*, Wiley, New York, **1994**, p. 602.
[26] M.-J. Kim, Y. I. Chung, Y. K. Choi, H. K. Lee, D. Kim, J. Park, *J. Am. Chem. Soc.* **2003**, *125*, 11494–11495.

[27] W. J. Moree, P. Sears, K. Kawashiro, K. White, C. H. Wong, *J. Am. Chem. Soc.* **1997**, *119*, 3942–3947.
[28] T. Ema, J. Kobayashi, S. Maeno, T. Sakai, M. Utaka, *Bull. Chem. Soc. Jpn.* **1998**, *71*, 443–453.
[29] a) T. Ema, R. Oyada, M. Fukumoto, M. Jittani, M. Ishida, K. Furuie, K. Yamaguchi, T. Sakai, M. Utaka, *Tetrahedron Lett.* **1999**, *40*, 4367–4370; b) T. Ema, K. Yamaguchi, Y. Wakasa, A. Yabe, R. Okada, M. Fukumoto, F. Yano, T. Korenaga, M. Utaka, T. Sakai, *J. Mol. Catal. B* **2003**, *22*, 181–192.
[30] M. Cygler, P. Grochulski, R. J. Kazlauskas, J. Schrag, F. Bouthillier, B. Rubin, A. Serreqi, A. Gupta, *J. Am. Chem. Soc.* **1994**, *116*, 3180–3186.
[31] a) J. C.-H. Chen, L. J. W. Miercke, J. Krucinski, J. R. Starr, G. Saenz, X. Wang, C. A. Spilburg, L. G. Lange, J. L. Ellsworth, R. M. Stroud, *Biochemistry* **1998**, *37*, 5107–5117; b) X. Wang, C. S. Wang, J. Tang, F. Dyda, X. C. Zhang, *Structure* **1997**, *5*, 1209–1218.
[32] C.-S. Chen, Y. Fujimoto, G. Girdaukas, C. J. Sih, *J. Am. Chem. Soc.* **1982**, *104*, 7294–7299.
[33] S. J. Weiner, P. A. Kollman, D. T. Nguyen, D. A. Case, *J. Comput. Chem.* **1986**, *7*, 230–252.
[34] H. M. Berman, J. Westbrook, Z. Feng, G. Gilliland, T. N. Bhat, H. Weissig, I. N. Shindyalov, P. E. Bourne, *Nucleic Acids Res.* **2000**, *8*, 235–242.

Received: December 19, 2003

